

sign depending upon the sense of the diagonal sequence, i.e., as the group III or group V element is the heavy one. Experimentally this has been found to be the case.<sup>1</sup>

If the surface state energy is assumed to change in the same direction as the (111) band gap and by approximately the same amount, one can estimate the barrier heights to be expected for the three compounds, using  $\phi_{Bn} = 2E_g/3$  as the unperturbed energy. The results of the procedure are shown in Fig. 1 together with the actual values for the other materials.

In spite of the empirical nature of this procedure, the results are in remarkable agreement with measured values. No doubt, with accurate wave functions for the surface state and an evaluation of the crystal potential

which can be made in the light of present experimental band structure studies, a sophisticated and enlightening calculation can be performed. Meanwhile, it is believed that the present study indicates a direction in which further fruitful investigations can be made.

#### ACKNOWLEDGMENTS

The authors wish to express their appreciation to D. Reynolds, M. Lorentz, W. Allred, R. Willardson, D. Bolger, T. Benedict, R. Wentorf, R. Ruehrwein, and L. Bailey for supplying materials used in this study. Pol Duwez in performing the x-ray diffractometer measurements, and H. M. Simpson for fabricating the samples.

## Lattice Dynamical Studies Using Absolute Measurements of the Lamb-Mössbauer Recoil-Free Fraction\*

W. A. STEVERT AND R. D. TAYLOR

*Los Alamos Scientific Laboratory, University of California, Los Alamos, New Mexico*

(Received 18 December 1963)

Absolute values of the recoil-free fraction  $f$  of the 14.4-keV  $\gamma$  rays of  $\text{Fe}^{57}$  are reported at temperatures from 4 to 1050°K.  $\text{Co}^{57}$ , the parent of  $\text{Fe}^{57}$ , is a dilute impurity in Au, Cu, Ir, Pd, Pt, Rh, and Ti. For intermediate temperatures the measured  $f$  is consistent with the calculations of Visscher, and Maradudin and Flinn when the impurity-host coupling constant is taken to be about the same as the host-host coupling constant. At the highest temperatures, the  $f$ 's of Au, Cu, and Pd fall off faster than simple theory would predict due to diffusion and anharmonicities. The results are compared with the anharmonic lattice theory of Maradudin and Flinn. Chemical and temperature-shift data are also reported.

#### INTRODUCTION

THE coupling between a Mössbauer nucleus and its surroundings enables the momentum of some of the  $\gamma$  rays to be absorbed by a large number of atoms, hence, for these  $\gamma$  rays there is almost no energy loss associated with the recoil. For this reason, studies of the Mössbauer emission provide an ideal method to investigate the nature of these coupling forces. The present study reports absolute measurements of  $f$  (the fraction of recoil-free emissions) and of the temperature shift (the temperature-dependent energy shift of the  $\gamma$  ray) in the case of an  $\text{Fe}^{57}$  nucleus as a dilute impurity in seven different host lattices. These hosts are elements in which the atomic size is very close to the atomic size of the Fe impurity; hence, we should expect the assumptions made in the Debye theory, and the refinements thereon by Visscher<sup>1</sup> and by Maradudin and Flinn<sup>2</sup> to have some validity. This is indeed the case for both the temperature shift and the  $f$  values in the

high-temperature region. At low temperatures the measured  $f$  values deviate slightly from theory.

#### EXPERIMENTAL METHOD AND RESULTS

##### General

The method we employ is to measure the Mössbauer spectrum of a source made up of  $\text{Co}^{57}$  in a nonmagnetic host metal using a single line absorber. The observed resonance strength  $F$  is

$$F = [N(\infty) - N(v_r)] / N(\infty) B = f f_{BL}. \quad (1)$$

$N(\infty)$  is the number of counts per unit time with the absorber moving at a sufficient velocity to prevent any resonance absorption,  $N(v_r)$  is the number of counts per unit time at the velocity  $v_r$  of the resonance peak, and  $B$  is the background correction.  $F$  is equal to the product of the recoil-free fraction of the source and the fractional absorption of these recoil free  $\gamma$  rays by the absorber (called the "blackness"  $f_{BL}$ ).

##### Equipment

For the low-temperature runs the source was mounted in a Dewar which had a pair of beryllium windows in

\* Work performed under the auspices of the U. S. Atomic Energy Commission.

<sup>1</sup> W. M. Visscher, Phys. Rev. **129**, 28 (1963).

<sup>2</sup> A. A. Maradudin and P. A. Flinn, Phys. Rev. **126**, 2059 (1962).

the bottom. The Be window which was in contact with the refrigerant liquid was soldered in place; this was made possible by an electropolated circumferential ring of nickel on the Be disk. The window was leak tight in He II. The high purity (99.9%) Be was found sufficiently free of  $\text{Fe}^{57}$  so as to have no measurable Mössbauer resonance. For high-temperature runs an electrically heated, water-jacketed oven was used. The thermocouple used for oven temperature measurements was checked against the known melting point of a National Bureau of Standards aluminum sample. The oven had mica and aluminum radiation shields and a Mylar window. A mixture of 20%  $\text{H}_2$  and 80% He was used in the furnace to prevent oxidation of the sources.

The absorbers were driven by a coupled loud speaker pair—one to drive the absorber and one to detect the motion. A 1-in. hole on axis through the driver assembly allowed the  $\gamma$  rays to pass through the absorber and into the detector. A feedback network in conjunction with this speaker pair produced a triangular velocity sweep at a frequency of 5.1 cps. A 400-channel pulse-height analyzer operating in the time mode stored the  $\gamma$ -ray pulses according to the time in the cycle at which they occurred. Thus, the spectrum was presented as counts received in a given time versus relative velocity of source and absorber.

The detector was an argon-methane filled proportional counter. Its energy resolution (11%) was sufficient to resolve the 14.4-keV  $\gamma$  ray from the  $K$  x ray (or  $L$  x ray of the high- $Z$  host materials) using a single-channel pulse-height analyzer. The non-14.4-keV background of the counter was due primarily to 123-keV  $\gamma$  rays emitted by the source. This background was determined by obtaining the counting-rate ratio with and without a 3/32-in. aluminum sheet inserted between the source and absorber, while the Mössbauer resonance was destroyed by a high absorber velocity. Since this sheet absorbed 99.8% of the 14.4-keV  $\gamma$  rays and 10% of the 123-keV  $\gamma$  rays, the percentage of non-14.4-keV  $\gamma$  rays could be determined by the counting rate ratio. This background correction was generally less than 15% and was accurately determined for each source at each temperature.

Another source of background was the recoil-free 14.4-keV  $\gamma$  rays which originated in the source but suffered Compton scattering or temperature diffuse scattering<sup>3</sup> before they passed through the resonant absorber; thus they lost their resonant character but still appeared in the counter as 14.4-keV  $\gamma$  rays. It was determined in a separate experiment that this leads to an appreciable correction in the case of the Dewar runs where Compton scattering took place in the Be windows.

<sup>3</sup> The effect of temperature diffuse scattering within the source may be calculated, taking as its intensity that given by B. Warren, *Acta Cryst.* **6**, 803 (1953), Eq. (1). Considering this effect in conjunction with competing electronic absorption, we derive a correction factor whose difference from unity is roughly proportional to  $T$ . It is 1.06 for Pd and Rh at 1000°K and 1.015 for the other hosts. This correction is included in the results quoted.

All Dewar  $F$  values have been increased by a factor of 1.027 to take this effect into account. It can be seen from Fig. 2 that the results in the furnace at chilled-water temperature (287°K) are consistent to within  $\pm 0.01$  of the results obtained in the Dewar at room temperature (297°K).

### Sources and Absorbers

Sources were prepared by diffusing into the host material 1 to 25 mCi of  $\text{Co}^{57}$ , which had been dried onto the host in the form of  $\text{CoCl}_2$  and reduced in place by  $\text{H}_2$ . Ir, Rh, and Au were commercial grade metals and the Ti, Pd, and Cu were special high-purity materials. Of these Au, Cu, Ti, Ir, and Pd were spectroscopically analyzed and showed less than 0.1% impurity before the Co diffusion.

Diffusion annealing in vacuum was done at 800–910°C for Au and Cu, and at 1100°C for the other hosts. That annealing was effective was shown by a decrease of the 14.4-keV  $\gamma$  rays relative to the 123-keV  $\text{Fe}^{57}$   $\gamma$  rays. The effect of self-absorption due to small quantities of stable  $\text{Fe}^{57}$  in the sources was less than 0.005 on the measurement of  $f$  in the worst cases and was neglected.

Several absorbers were used in this study. An enriched iron absorber containing 1 mg  $\text{Fe}^{57}/\text{cm}^2$  was used for velocity calibration and for determining linewidths. Absolute  $f$  values were determined using a pair of very broad absorbers; these absorbers were made up of a mixture of  $\text{Fe}^{57}$  enriched lithium and ammonium ferric fluorides according to a recipe of Housley, Erickson, and Dash,<sup>4</sup> and each absorber contained 20 mg  $\text{Fe}^{57}/\text{cm}^2$ . Relative  $f$  values were obtained using a moderately broad Fe-Ti absorber. The 0.1 Fe-0.9 Ti alloy was 0.002 in. thick and contained 2 mg  $\text{Fe}^{57}/\text{cm}^2$ .

### Determination of the Recoil-Free Fraction

In order to measure absolute  $f$  values, an absorber with a known  $f_{BI}$  is required. The special properties of the lithium-ammonium ferric fluoride absorbers (referred to as Li-NH<sub>4</sub> absorbers) make this readily possible. The ammonium ferric fluoride has a pair of broad lines for its absorption pattern; the lithium ferric fluoride has a single broad-line pattern, which falls between the pair of lines of the ammonium salt. Combined in the proper proportions the mixed salts have a broad, flat-topped absorption pattern. The full width at half-maximum of this pattern is 3.1 mm/sec or about 30 times the linewidth of our narrow line sources.

Because the Li-NH<sub>4</sub> absorbers are very thick, they absorb essentially all of the Mössbauer  $\gamma$  rays lying between  $\pm 15$  source linewidths of the line center. This encompasses all of the source Mössbauer  $\gamma$  rays, except 2.5% lying in the wings of the Lorentzian, hence making

<sup>4</sup> R. M. Housley, N. E. Erickson, and J. G. Dash (to be published).

the absorbers 97.5% black. Adjusting for the fact that the absorption in the flat top is not perfect, we obtain  $f_{BI}=0.97$ .<sup>5</sup> Measurements using these absorbers were carried out on most of the sources at 4 and 297°K, and the source  $f$  values were thus obtained by dividing the observed  $F$  by 0.97.

Since the absolute value of  $f$  is now known for most of the sources at at least one temperature, we can obtain  $f_{BI}$  for the Fe-Ti absorber appropriate to each source and use this absorber for the measurements at other temperatures, using Eq. (1), i.e.,  $f_{BI}=F/f$ . The advantage here lies in the smaller electronic absorption cross section for the Fe-Ti absorber, allowing higher counting rates with smaller background corrections.

The absorption pattern for the Fe-Ti absorber and Cu source is a broad single line, with a somewhat flattened top on it; the linewidth is about 0.8 mm/sec. For the narrow line sources  $f_{BI}=0.92$ , for the wide line sources  $f_{BI}=0.88$ .

### Source Linewidths

The observed linewidths  $\Gamma$  as a function of temperature for six of the sources and the 75% enriched pure Fe absorber are given in Fig. 1. The data are presented as the ratio of  $\Gamma/\Gamma_t$ , where  $\Gamma_t$  is the theoretical linewidth of an ideal source and absorber corrected for broadening due to absorber thickness. The weak inner pair of absorption lines of the Fe hyperfine spectrum was used and the internal conversion coefficient was taken to be<sup>6</sup> 9.5, and the half-life of the first excited state was taken to be<sup>7</sup>  $1.0 \times 10^{-7}$  sec in calculating  $\Gamma_t$ .  $\Gamma_t$  was determined to be 0.23 mm/sec. The observed broadening in excess of  $\Gamma_t$  is due to excess linewidth in the source, variations in the hyperfine field in various magnetic domains in the absorber, and spurious vibrations in the absorber drive. It is felt that no significant temperature dependence of  $\Gamma$  is shown so the  $f_{BI}$  used with each source includes no temperature-dependent linewidth correction.

### Results

The absolute  $f$  values at 293°K are given in Table I for Fe<sup>57</sup> in the seven host metals.<sup>8</sup> Also the  $f$  values at

<sup>5</sup> We can determine this adjustment in several ways. The most accurate way is to place a nonmoving Li-NH<sub>4</sub> absorber in front of a source, then run an ordinary Mössbauer spectrum using a Fe-Ti absorber. When this is done, no Mössbauer resonance peak appears (to within statistical error) because the source Mössbauer  $\gamma$  rays are absorbed by the Li-NH<sub>4</sub> absorber. Because the properties of the Fe-Ti absorber are known, this argument can be made quantitative and an upper limit of 0.5% can be put on the transparency of the absorber to those Mössbauer  $\gamma$  rays with an energy lying within the flat part of the absorption spectrum. The same conclusion is reached by running a spectrum using the two Li-NH<sub>4</sub> absorbers and noting that the same resonance strength  $F$  is observed.

<sup>6</sup> A. H. Muir, Jr., E. Kankeleit, and F. Boehm, Phys. Letters 5, 161 (1963).

<sup>7</sup> H. Frauenfelder, *The Mössbauer Effect* (W. A. Benjamin, Inc., New York, 1962).

<sup>8</sup> Titanium data are not available above 250°C. The source was destroyed at 500°C in the 0.2 hydrogen-0.8 helium furnace atmosphere. Iridium data are not available below room temperature

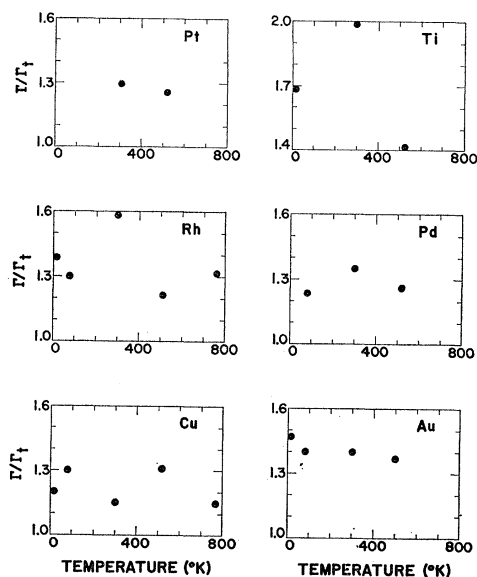


FIG. 1. Observed linewidths  $\Gamma$  divided by the theoretical linewidth  $\Gamma_t=0.23$  mm/sec for the various sources and the Fe absorber. Not shown is Ir for which  $\Gamma/\Gamma_t=2.2$  at 298°K.

4 and 773°K are listed. Data on other temperatures are not tabulated, but may be found in Fig. 2. For most of the sources the estimated uncertainty is  $\pm 1.5\%$  of the absolute  $f$  value due to the uncertainty in  $f_{BI}$ ; for Ir and Ti this uncertainty becomes  $\pm 2.5\%$  reflecting the increased uncertainty in  $f_{BI}$  accompanying the increased source linewidth. In addition there is a statistical error of  $\pm 0.005$ , for all data except Pt at 4 and 75°K where this error is  $\pm 0.04$ .

The rest of Table I lists the observed energy shift of the 14.4-keV  $\gamma$  ray at several temperatures for the various hosts. A zero chemical shift is taken as the case of a

TABLE I. Some measured absolute  $f$  values and shifts relative to Fe<sup>57</sup> in Fe at 298°K in various host metals at several temperatures. A positive shift means higher  $\gamma$ -ray energy.

Host	Observed recoil-free fraction			Observed shift, $\Delta E/E$ in units of $10^{-13}$		
	4°K	293°K	773°K	4°K	298°K <sup>b</sup>	1023°K
Ir	...	0.807	0.585	...	7.5	-10.4
Rh	0.875	0.785	0.555	8.3	3.8	-13.8
Pt	0.851	0.729	0.432	17.0	12.0	-6.2
Cu	0.917	0.727 <sup>a</sup>	0.368	12.2	7.8	-9.0
Pd	0.813	0.652 <sup>a</sup>	0.345	11.5	6.8	-11.8
Au	0.867	0.598	0.241	26.4	20.8	1.6
Ti	0.818	0.470	...	6.2	-1.0	...

<sup>a</sup> As a recheck, second Cu and Pd sources were prepared. While they had different impurity concentrations from the original sources, they were still quite pure and gave  $f$  values of 0.715 and 0.66, respectively, at 297°K.

<sup>b</sup> To the extent that these data lie in the linear part of the high-temperature region, this is the chemical shift at 298°K.

due to the observation of spontaneous magnetic hyperfine splitting at 4°K for 40% of the Fe<sup>57</sup> atoms. This is due to an insufficiently hot anneal of the high melting point source. In this, our worst source, the Co concentration may have been as high as 1%, thus making interactions between magnetic impurities appreciable at low temperatures.

Co<sup>57</sup> in Fe source and a Fe<sup>57</sup> in Fe absorber, both at 298°K. Independent experiments, where an absolute velocity calibration is available, show that indeed the maximum Mössbauer absorption for this case occurs at Doppler velocity of zero. The shift data at several temperatures presented in Table I are derived from the velocity shift in the Mössbauer spectra of the sources analyzed by a Fe<sup>57</sup> in Fe absorber at 298°K and then relating this shift to the energy shift by  $\Delta E/E = \Delta v/c$ , where  $c$  is the velocity of light. The Doppler drive was calibrated using the known Mössbauer spectrum of Fe<sup>57</sup> in Fe.<sup>7</sup> This method of calibration can lead to systematic errors as large as  $\pm 1\%$ , due to the fact that the actual hyperfine field of the thin Fe absorber is influenced by small demagnetizing effects. Data at other temperatures will be found in Fig. 3. The standard error of all the data is  $0.6 \times 10^{-13}$ , in addition to the  $\pm 1\%$  just mentioned.

### THEORY

#### General

The probability ( $f$ ) of recoil-free  $\gamma$ -ray emission is given by

$$f = \langle i | \exp(i\mathbf{\kappa} \cdot \mathbf{r}) | i \rangle^2, \quad (2)$$

where the matrix element is calculated between initial and final states of the lattice which are identical (no energy change of the lattice at the expense of the  $\gamma$  rays). Here  $\mathbf{r}$  is the position of the emitting nucleus and  $\mathbf{\kappa}$  is the wave vector of the  $\gamma$  ray ( $|\mathbf{\kappa}| = \kappa = 2\pi/\lambda$ , where  $\lambda$  is the  $\gamma$ -ray wavelength). If the physical situation meets certain requirements<sup>9</sup> we can write Eq. (2) as

$$f = \exp(-\kappa^2 \langle x^2 \rangle_{av}), \quad (3)$$

where  $\langle x^2 \rangle_{av}$  is the mean-squared displacement of the emitting atom from its equilibrium position (along the direction of emission) as it vibrates in the lattice due to its zero point and thermal energy. The models we will discuss meet these requirements.

The frequency of the Mössbauer line is dependent on temperature through the second-order Doppler shift.

$$\frac{\Delta E}{E} = \frac{\langle v_{T_1}^2 \rangle_{av} - \langle v_{T_2}^2 \rangle_{av}}{2c^2} = \frac{\epsilon_{T_1} - \epsilon_{T_2}}{Mc^2}. \quad (4)$$

Here  $\Delta E/E$  is the fractional change of the  $\gamma$ -ray energy as the temperature is changed from  $T_1$  to  $T_2$ ;  $\langle v_{T_2}^2 \rangle_{av}$  is the mean-squared velocity of the emitting nucleus and

$\epsilon_T$  is the mean kinetic energy of the nucleus at temperature  $T$ .  $M$  is the mass of the nucleus.

It is important to note that when the temperature is high enough,  $\epsilon_T = \frac{3}{2}kT$  (within the applicability of equipartition of energy). Also, it is assumed that in Eq. (4) the chemical shift associated with the overlap of nuclear and electronic wave functions is temperature-independent.

#### Debye Theory

As a first approximation one considers a perfect lattice made up of identical nuclei of mass  $M$ . The eigenstates of the system are longitudinal and transverse phonons. The number of eigenstates per unit angular frequency increment is given by  $n(\omega) \propto \omega^2$  for  $\omega < \omega_m$  and  $n(\omega) = 0$  for  $\omega > \omega_m$ . The choice of  $\omega_m$  is such that there be  $3N$  phonons in a lattice made up of  $N$  atoms. The Debye temperature  $\theta_D$  is given by  $k\theta_D = \hbar\omega_m$ . Each mode has a statistical thermal energy  $U_T(\omega)$  and an  $\langle x^2 \rangle_{av} = U/M\omega^2$ . Assuming incoherence of  $\langle x^2 \rangle_{av}$  from various modes:

$$\langle x^2 \rangle_{av}(T) = \int_0^\infty \frac{U_T(\omega)n(\omega)d\omega}{M\omega^2}. \quad (5)$$

The result is the Debye-Waller factor

$$f = \exp(-\kappa^2 \langle x^2 \rangle_{av}) = e^{-2W}, \quad (6)$$

$$2W = -\frac{3}{2} \frac{R}{\theta_D} \left\{ 1 + 4 \left( \frac{T}{\theta_D} \right)^2 \int_0^{\theta_D/T} \frac{x dx}{e^x - 1} \right\}. \quad (6a)$$

For  $T > \theta_D/2$

$$2W = 6RT/\theta_D^2, \quad (6b)$$

$R = E^2/2Mc^2$  and is the recoil energy of an unbound emitting nucleus. In the case of Fe<sup>57</sup>,  $R = 22.6^\circ\text{K}$ .

A curve of the type defined by Eqs. (6) is shown in Fig. 2 for the case of Ti;  $\theta_s$ , the  $\theta$  derived from these  $f$ -value measurements, is 237°K.

The second-order Doppler shift may be derived from Eq. (4) where  $\epsilon_T$  is  $\frac{1}{2}U_T$ .  $U_T$  is the total energy of the lattice vibrations at temperature  $T$  according to the Debye theory. The behavior of  $\Delta E/E$  at high temperatures was given in the previous section to be proportional to  $T$ . This limiting behavior may be seen in Fig. 3, where the solid curves are those appropriate to the Debye theory. The higher  $\theta_s$  is, the more severe is the deviation from a straight line at low temperatures.  $\theta_s$  refers to the  $\theta$  derived from the shift measurements. These solid curves represent the best fit of the Debye theory to experiment with  $\theta_s$  taken as a variable parameter; the shape of the curve is not very sensitive to  $\theta_s$ , hence  $\theta_s$  is determined only roughly.

#### Impurity Theories

Visscher<sup>1</sup> takes as his model a simple cubic lattice with atoms bound by harmonic potentials. Also he assumes shear spring constants equal to the compressive

<sup>9</sup> These requirements are considered in a recent paper by H. Lipkin [Ann. Phys. (N. Y.) **26**, 115 (1964)]. Essentially he finds that Eq. (3) is valid if the lifetime of the excited vibrational state of the crystal is short compared to the nuclear lifetime (0.14  $\mu\text{sec}$ ). A long lifetime state, such as might conceivably be associated with a localized impurity mode, would give rise to a correction factor to Eq. (3) involving a Bessel function of imaginary argument, which at high temperatures would tend to increase the value of  $f$  over the exponential decrease shown in Fig. 3. Such a long lifetime seems unlikely due to relaxation with the lattice vibrations having a characteristic period of  $10^{-14}$  sec.

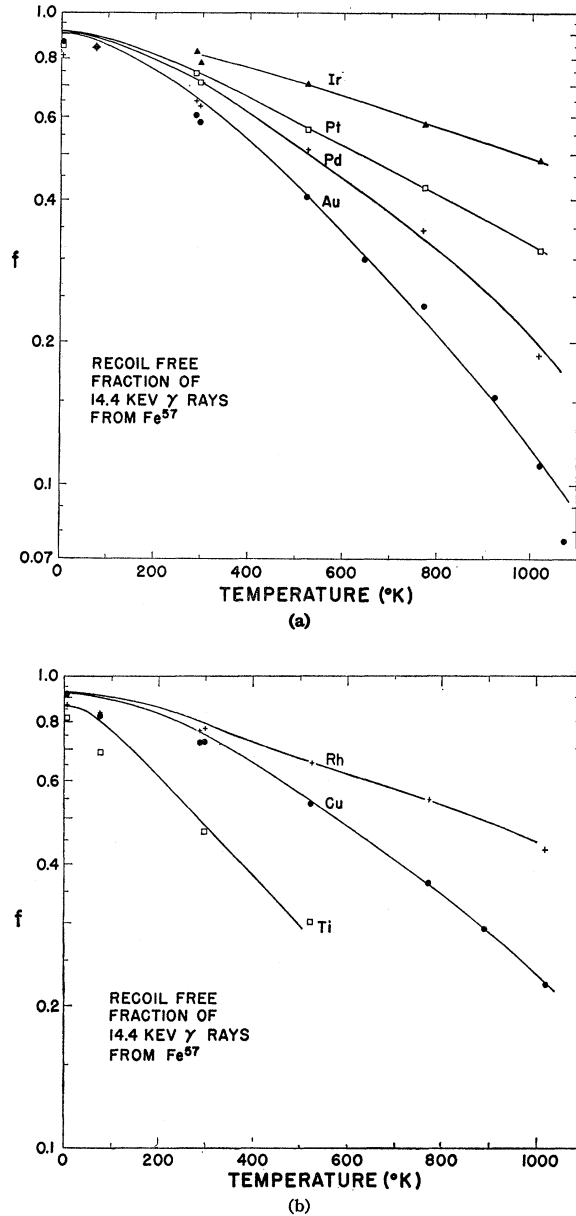


FIG. 2. Fraction of recoil-free  $\gamma$  rays from  $\text{Fe}^{57}$  in various hosts. The curves are the best fit Debye-Waller curves, modified to take into account anharmonic effects. The parameters used in the fit are given in Table II.

spring constants—i.e., if the atom at the origin is moved a given distance in the positive  $x$  direction with respect to its equilibrium position, the forces on its neighbors on the  $x$ ,  $y$ , and  $z$  axes are all equal and in the positive  $x$  direction. The four parameters in this theory are the masses of the impurity and the host ( $\mu'$  and  $\mu$ ), and the host-impurity and host-host spring constants ( $\gamma'$  and  $\gamma$ ), i.e., the second derivatives of the interatomic potential. The result is that  $f(T)$  is approximated quite well by the Debye theory above room temperature

except  $\mu'$  and  $\gamma'$  determine the  $R$  and  $\theta$  of the theory instead of  $\mu$  and  $\gamma$ .

From the Debye theory  $\theta_D \propto (\gamma/\mu)^{1/2}$  for the host. However, we want an effective  $\theta_{\text{eff}} \propto (\gamma'/\mu')^{1/2}$ . We see that  $\theta_{\text{eff}} = (\mu/\mu')^{1/2} (\gamma'/\gamma)^{1/2} \theta_D$ . All these parameters are known except  $\gamma'/\gamma$ .<sup>10</sup>

The Einstein single-particle model approximates the impurity as an oscillator in a spherical harmonic well. The oscillator frequency is  $\omega_E = k\theta_E/\hbar$ , where  $\theta_E$  is the Einstein temperature. Because of coupling between the oscillator and the lattice, the oscillator will jump from one level to another many times during the nuclear lifetime. Hence, we are permitted to use Eq. (3).<sup>9</sup> The resulting  $f(T)$  is the same as the Debye  $f(T)$  in the high-temperature region (if  $\theta_E = \theta_D/\sqrt{3}$ ). At  $T=0$ , however, the Einstein  $f(T)$  will be about 0.03 lower than the equivalent Debye  $f(T)$  in the range  $100^\circ\text{K} < \theta_D < 500^\circ\text{K}$ . This model, as well as the Visscher model, which has the same behavior, fits the experimental data better than the Debye model in the low-temperature region. It is perhaps surprising that the three models give so nearly the same  $f(T)$  when the phonon spectra  $n(\omega)$  are so different. Too, the theoretical temperature shifts in the Visscher and Einstein model are almost the same as for the Debye model.

Maradudin and Flinn have calculated the recoilless fraction in the high-temperature limit considering nearest-neighbor interactions in a fcc lattice. As with Visscher's theory, it is possible to define a  $\theta_{\text{eff}}$ ; in this case<sup>11</sup>

$$\theta_{\text{eff}} = \theta_D (\mu/\mu')^{1/2} \left[ 1 + 0.60 \left( \frac{\gamma - \gamma'}{\gamma} \right) + 0.74 \left( \frac{\gamma - \gamma'}{\gamma} \right)^2 + \dots \right]^{-1/2}, \quad (7)$$

### Anharmonic Effects

All the previous theories of this section predict that for high temperatures  $\ln f \propto T$ . However, Maradudin and Flinn<sup>12</sup> calculate the effect of anharmonic binding forces on  $f$  in the case of a pure crystal. They find that

$$\ln f = -mT(1 + \epsilon T + \delta T^2 + \dots). \quad (8)$$

Here  $\delta$  is expected to be very small and will be neglected,

<sup>10</sup> Using a different model, almost identical results have been obtained by Y. Kagen and Y. Iosilevskii, *Zh. Eksperim. i Teor. Fiz.* **44**, 284 (1963) [English transl.: *Soviet Phys.—JETP* **17**, 195 (1963)]. See also H. Lipkin, *Ann. Phys. (N.Y.)* **23**, 28 (1963).

<sup>11</sup> Neither Visscher's or M. & F.'s theories are formulated in terms of  $\theta_{\text{eff}}$ , instead they are formulated in terms of  $\gamma$  and  $\gamma'$ . However, to relate these theories to experiment a value of  $\gamma$  is required, leaving our only free parameter  $\gamma'$ . For our purposes the best measure is  $\theta_D$  because it represents an average over all frequencies of phonons, while other measures represent only the very low frequency end of the phonon spectrum. Defining  $\theta_{\text{eff}}$ , then, allows us to interrelate the  $f$  values and the host specific heat measurements, modified by the Visscher and M. & F. theory to allow for impurity-mass and binding-constant changes.

<sup>12</sup> A. A. Maradudin and P. A. Flinn, *Phys. Rev.* **129**, 2529 (1963).

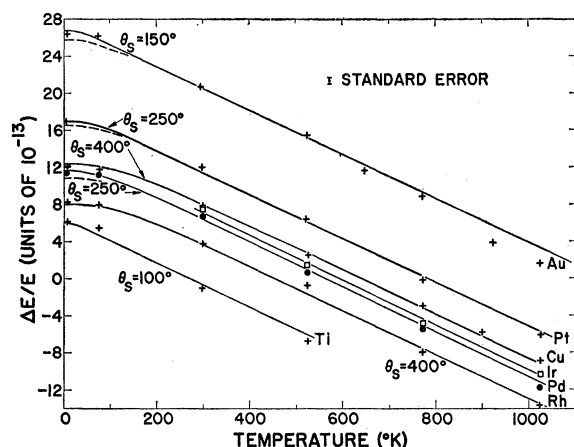


FIG. 3. Combined temperature and isomeric shift ( $\Delta E/E$ ) of  $\text{Fe}^{57}$  in a host relative to  $\text{Fe}^{57}$  in Fe. Curves are the best fit Debye theory curves. The dashed curves are the Debye theory with  $\theta_D$  taken from the measured  $f$  of Table II. For elements with no dashed curves, the difference is too small to show.

and  $\epsilon$  is the parameter leading to the slight downward curvature of the curves in Fig. 2. The parameter  $m$  is the coefficient of  $T$  appearing in the right-hand side of Eq. (6b). While this theory, like the Debye theory, makes no allowance for an impurity, it is nevertheless instructive to compare its results with the observed behavior. The quantity  $\epsilon$  is determined by  $d\gamma/dr$  and  $d\gamma^2/dr^2$ , which may be obtained from the expansion coefficient and an assumed interatomic pair potential  $\varphi(r)$ , respectively. The sign of  $\epsilon$  is predicted as positive; however, a different assumption about the shape of  $\varphi(r)$  would lead to a negative  $\epsilon$  and an upward curvature of the curves of Fig. 2. Anharmonic effects have previously been seen in the case of tin.<sup>13</sup>

## DISCUSSION

### Anharmonicities

In Fig. 2 it can be seen that the anharmonic theory of the preceding section with the variable parameters  $\theta_{\text{eff}}$  and  $\epsilon$  accounts for the high-temperature behavior to within  $\pm 0.01$ . The Einstein or Visscher models anticipate the anomalous low-temperature behavior seen in that figure. We can now discuss how the quantitative prediction of the theories compare with experiment.

Table II shows the values of  $\epsilon$  calculated for the pure metal, using Maradudin and Flinn's theory and a Morse potential  $\varphi(r)$ . The measured  $\epsilon$ 's are considerably larger than the predicted values in all cases. One reason lies in differences in the atomic sizes of the impurity atom and the host, leading to anharmonic impurity-host binding forces. (Except for copper all of the host atoms reported here are 5% to 10% larger in radius than iron atoms in iron.)

<sup>13</sup> A. J. F. Boyle, D. St. P. Bunbury, C. Edwards, and H. E. Hall, Proc. Phys. Soc. (London) **77**, 129 (1961).

TABLE II. Comparison between the calculated and measured anharmonicities; also the binding constant ratios ( $\gamma'/\gamma$ ) derived from two different theories using the lattice-dynamical parameters of columns 4 and 6.

Host	Anharmonic coefficient $\epsilon$ ( $^{\circ}\text{K}^{-1}$ )	$\theta_D$ of host <sup>a</sup> $^{\circ}\text{K}$	$\theta_{\text{eff}} =$ $(\mu/\mu')^{1/2}\theta_D^b$ $^{\circ}\text{K}$	$\theta_f$ $^{\circ}\text{K}$	$\gamma'/\gamma$ from Visscher's theory	$\gamma'/\gamma$ from M & F (2) theory	
Ir	$0.3 \times 10^{-4}$	$0.92 \times 10^{-4}$	285	522	457	0.77	0.85
Rh	0.4	0.67	350	470	427	0.83	0.90
Pt	0.4	0.97	233	431	363	0.71	0.81
Cu	1.0	6.85	343	362	397	1.20	1.4 <sup>c</sup>
Pd	0.5	6.14	275	376	373	0.98	0.98
Au	0.6	7.00	164	305	329	1.16	1.4 <sup>c</sup>

<sup>a</sup> Measurements of  $\theta_D$  vary from 280 to 430 $^{\circ}\text{K}$  for Ti.

<sup>b</sup> Calculated values using  $\gamma'/\gamma=1$ .

<sup>c</sup> These figures are questionable; for  $\gamma'/\gamma=1.4$  the higher order terms of the power series of Eq. (7) may be important.

However, there is another way to look at the problem. We know that even in pure metals the elastic constants decrease with increasing temperature<sup>14</sup>; while data are not available to 1000 $^{\circ}\text{K}$ , extrapolation of the room-temperature results to 1000 $^{\circ}\text{K}$  gives a 25% decrease in  $c_{44}$  for Cu and Au. This shear modulus is a good measure of  $\gamma$  because it is not greatly affected by the electronic contribution to the elastic properties. The short-wavelength phonons which play a major role in determining  $f$  at high temperatures<sup>15</sup> are also unaffected by the electronic contribution to the spring constants since phonon wavelengths are shorter than electronic mean-free paths. This 25% decrease in  $\gamma$  is equivalent to a 12% decrease in  $\theta_{\text{eff}} \propto \sqrt{\gamma}$  and on the basis of Eq. (6) accounts for 50% of the observed high-temperature falloff in Fig. 2.

### Diffusion

Based on measured diffusion constants for Fe in Au, an Fe atom will move from one lattice site to another every<sup>16</sup> 1.3  $\mu\text{sec}$  at 1000 $^{\circ}\text{K}$ ; the mean nuclear lifetime is 0.14  $\mu\text{sec}$ . Hence 11% of the Fe atoms in gold at 1000 $^{\circ}\text{K}$  will move a distance equivalent to several wavelengths during their lifetimes and it is reasonable that the measured  $f$  will be decreased<sup>17</sup> for gold above 1000 $^{\circ}\text{K}$  because of diffusion either through line broadening, or the creation of side peaks, as theoretically predicted, or through an unpredicted actual decrease in  $f$ . For all

<sup>14</sup> H. B. Huntington, in *Solid State Physics*, edited by F. Seitz and D. Turnbull (Academic Press Inc., New York, 1958), Vol. 7, p. 322.

<sup>15</sup> Other elastic constants, measured by ultrasonics or static compressibility, involve changes in volume at low frequencies, hence the electrons will contribute since they resist static compression.

<sup>16</sup> D. Lazarus, in *Solid State Physics*, edited by F. Seitz and D. Turnbull (Academic Press Inc., New York, 1960), Vol. 10, p. 71. Also W. Seith, *Diffusion in Metallen* (Springer-Verlag, Berlin, 1955), p. 49.

<sup>17</sup> See the discussion of A. J. F. Boyle and W. Marshall, in *Proceedings of the Second International Conference on the Mössbauer Effect*, edited by A. H. Schoen and D. M. J. Compton (John Wiley & Sons, Inc., New York, 1962), pp. 81-84. Also, A. J. F. Boyle and H. E. Hall, Rept. Progr. Phys. **25**, 441 (1962).

other materials used the diffusion times of Fe are expected to be much greater,<sup>16</sup> and no effect is observed.

Because of low  $f$  values it was impossible to obtain accurate linewidth data at 1000°K where diffusion is important. Diffusion line broadening, as predicted by Singwi and Sjölander,<sup>18</sup> if present, is less than one natural linewidth (0.1 mm/sec).

### Measured $\theta_f$ 's

Table II compares the  $\theta_{\text{eff}}$ 's predicted if  $\gamma'/\gamma = 1$  to  $\theta_f$ , the  $\theta$  derived from  $f$ -value measurements. Then  $\gamma'/\gamma$  is taken as a variable parameter and the last two columns tabulate the values of that parameter which are required to make the calculated  $\theta_{\text{eff}}$  equal  $\theta_f$ . If we recall that iron is a smaller atom than any of the hosts, except copper, the predominance of  $\gamma'/\gamma$  values less than unity is not surprising. The large  $\gamma'/\gamma$  for Au, along with its large chemical shift (Table I), makes it anomalous to the over-all pattern.

### Low-Temperature Behavior

In Fig. 2 the low-temperature data  $T \leq 200^\circ\text{K}$  lie below the extrapolated Debye curves. This is in qualitative agreement with the Visscher and Einstein models. However, the observed deviation is larger than predicted—these models predict a deviation of about 0.03 near absolute zero, where our results lie about 0.05 below the extrapolated Debye curves. The difference of 0.02 is barely outside of the experimental accuracy, but may indicate an aspect of the problem which is not understood.

### Temperature and Chemical Shifts

Figure 3 illustrates the chemical- (isomeric) shift and temperature-shift data. The solid theoretical curves are drawn assuming the Debye theory and that the chemical shift, associated with differences of  $|\psi(0)|^2$  between the source and absorber, is temperature-independent.  $|\psi(0)|^2$  is the probability per unit volume of finding an electron at the nucleus. It has been demonstrated<sup>19</sup>

<sup>18</sup> K. S. Singwi and A. Sjölander, Phys. Rev. **120**, 1093 (1960).

<sup>19</sup> R. V. Pound, G. B. Benedek, and R. Drever, Phys. Rev. Letters **7**, 405 (1961).

that  $|\psi(0)|^2$  is dependent on volume, for Fe<sup>57</sup> in Fe at room temperature, and hence as the temperature is increased, the expansion of the Fe would lead to a 6% decrease in the slope of the data in Fig. 2. This is not observed in our data or in the case of Fe<sup>57</sup> in iron<sup>20</sup> in the region where we can accurately predict  $\langle v^2 \rangle_{\text{av}}$ , namely above 500°K. (Our host metals have expansion coefficients which vary from 50 to 150% that of iron.) Presumably the observed absence of this 6% decrease in slope is due to some compensating temperature-dependent, volume-independent, chemical-shift mechanism.

It will be noticed by comparing Fig. 3 to Table II that  $\theta_s$  tends to be smaller than  $\theta_f$ . If the Einstein model were used, the measured  $\theta_E$  based on  $f$  values and measured  $\theta_E$  based on shifts would be in better agreement with no systematic trend. This may indicate the importance of a localized mode, as per Visscher's calculations.

### CONCLUSION

The downward curvature of the measured  $f$  values at high temperatures is 3 to 10 times larger than the theoretical predictions of Maradudin and Flinn would indicate. It is twice as large as predicted from changes of  $\gamma$  due to weaker force constants at higher temperatures in two cases where these numbers are known.

Applying the calculations of Maradudin and Flinn, and Visscher, with  $\gamma'/\gamma$  taken as a variable parameter we can fit the experimental data for the different hosts with  $0.7 < \gamma'/\gamma < 1.4$ . When  $\mu'/\mu < 0.6$  ( $\gamma'/\gamma \approx 1$ ), Visscher expects the  $f$  values at low temperatures to fall below the Debye curves due in part to the creation of a localized mode. Such a trend is seen in Fig. 2.

### ACKNOWLEDGMENTS

The expert assistance of D. R. F. Cochran in source preparation is gratefully acknowledged. This work was stimulated by discussions with P. P. Craig. Discussions with J. G. Dash, T. Kitchens, W. C. Overton, and W. M. Visscher have been most valuable.

<sup>20</sup> R. S. Preston, S. S. Hanna, and J. Heberle, Phys. Rev. **128**, 2207 (1962).